V European Conference on Computational Fluid Dynamics
ECCOMAS CFD 2010
J. C. F. Pereira and A. Sequeira (Eds)
Lisbon, Portugal, 14–17 June 2010

NUMERICAL INVESTIGATION OF LAMINAR BURNING VELOCITIES FOR VARIOUS PREMIXED GASEOUS HYDROGEN/HYDROCARBON/AIR MIXTURES

Hugo M. Campelo[*], Siva P.R. Muppala[†], Jennifer X.Wen[††] and B. Manickam [+]

[*]Faculty of Engineering, Kingston University
now with Efacec, Energia, S.A., Porto, Portugal
e-mail: hugo.campelo@gmail.com

[†, ††]Faculty of Engineering, Kingston University
Friars Avenue, Roehampton Vale, London SW15 3DW

[+]Institute for Technical Combustion, Leibniz Hannover University, Hannover, Germany

Keywords: Premixed laminar flame, Blended mixtures, 1-D simulation, Laminar burning velocity.

Abstract. *The enhanced combustion properties of hydrogen as well as worldwide concerns due to global warming are acting together as the major driving force to a future hydrogen-based economy. However this will not be a step change and the blends of hydrogen and hydrocarbons must be looked as a transition solution to a purely hydrogen-based economy [1]. In the present study, numerical investigations of a wider range of fuel/air mixtures which includes H_2-hydrocarbon blends have been carried out for the unstretched laminar burning velocities, S_{L0} at STP conditions using detailed reaction mechanisms. For this purpose, different reaction mechanisms are combined with the combustion simulation package Cosilab [2]. Comparative studies with experimental data from several independent investigations show that San Diego mechanism [3] predicts S_{L0} of H_2/air mixtures very well while Konnov v0.5 [4] is the most valid mechanism for CH_4/air mixtures. QMech [5] shows good agreement for C_3H_8/air mixtures. For H_2/CH_4/air mixtures of overall equivalence ratio 1.0, kinetic mechanisms show a splitting behaviour for varied concentration levels of blended fuel hydrogen. For mixtures with volume concentrations of H_2 (Vol. H_2) < 60%, QMech predicts reasonable results while for Vol. $H_2 \geq 60\%$ Appel [6] is comparatively better. QMech also shows valid predictions for H_2/C_3H_8/air mixtures especially for equivalence ratios between 0.6 and 1.0. For H_2/CO/air mixtures satisfactory agreement is found with CMech [7]. An extended evaluation of the influence of carbon dioxide in the latter mixture is conducted which shows that S_{L0} decreases almost linearly with increasing quantities of carbon dioxide.*

1 INTRODUCTION

Hydrogen is not a primary source so it must be manufactured at significant costs and with energy consumption. Moreover his challenge was addressed and several pathways were already identified in order to develop a purely hydrogen based economy [2]. Consequently this will not be an abrupt change and hydrocarbon-hydrogen blends must be looked on one hand as a transition solution into a cleaner energy source [1] and on the other hand as way of preventing flame instabilities in today's combustors [3].
The major driving force comes from the concerns (and possible costs) due to global warming but also because hydrogen may allow significant enhancements in the operability ranges of many combustion devices (e.g. piston engines). The operation of such devices under lean conditions is advantageous in terms of achieving both high thermal efficiency and low NOx emissions, but lean flames present inherent instabilities [3]. Nevertheless hydrogen combustion is characterized by increased mean local burning velocities, especially noticeable under ultra lean conditions, due to molecular transport effects and stretch that strongly affect the local burning velocity near the convex zone of the flame [4] producing efficient operations and reducing ignition lag [5].

Besides combustor's design one of the biggest commitments with hydrogen potential as clean fuel comes for example from the Dutch government who is considering hydrogen addition to the natural gas grid, which feeds all household burners [6].

One of the most important intrinsic properties of any combustible mixture is its laminar burning velocity and its dependence on variables such as pressure, temperature and mixture composition. Many practical examples of combustion (from water gas heaters to engines) rely on turbulent flames which share some of their characteristics with laminar flames [7]. In fact, the prediction of the turbulent flame speed has been challenging for the combustion community for many years [8] and the laminar burning velocity is a fundamental input in one of the most important approaches where such flames are considered as a set of laminar-like flamelets [9].

In the present investigation we aim to identify the best kinetic mechanisms that should be used to predict laminar burning velocities of several hydrocarbon-air-flames and also to study the dilution effect of the synthesis gas with carbon dioxide. All the results computations were made using the commercial laminar flame code Cosilab [10]. Steady state simulations of freely planar propagating flames are used through all the present work unless explicitly stated. The scope of this study is limited to flames at atmospheric pressure and ambient temperature (1 bar and 298K, respectively).

2 NUMERICAL METHODS –SPHERICAL VERSUS FREELY PROPAGATING FLAMES

Here the adjective 'freely' implies that such flames are free from external disturbances as near-by walls and burner-nozzles or rods. We are dealing with one-dimensional 'low-Mach-number reactive' flows in stream-tubes, tubes or pipes with variable cross-sectional area. Here the adjective 'low-Mach-number' means low flame speeds (deflagrations) and inviscid flows with spatially uniform pressure.

Thus the governing equations used to model the above mentioned flames are the continuity equation,

$$\frac{\partial \rho}{\partial t} + \frac{1}{A}\frac{\partial}{\partial x}(\rho v A) = 0 \qquad \text{(I)}$$

The species mass conservation equations for each species

$$\rho\left(\frac{\partial Y_i}{\partial t}+v\frac{\partial Y_i}{\partial x}\right)=-\frac{1}{A}\frac{\partial}{\partial x}(j_i A)+w_i \tag{II}$$

The energy equation

$$\rho C_p\left(\frac{\partial T}{\partial t}+v\frac{\partial T}{\partial x}\right)=\frac{1}{A}\frac{\partial}{\partial x}\left(\lambda A\frac{\partial T}{\partial x}\right)-\frac{dT}{dx}\sum_{i=1}^{n}j_i C_{p,i}-\sum_{i=1}^{n}h_i w_i+\frac{dp^0}{dt}-\frac{1}{A}\frac{\partial}{\partial x}(q_r A)+A_{eq}h(T-T_0) \tag{III}$$

and the ideal-gas equation of state

$$p^0=\rho\overline{R}T\sum_{i=1}^{n}\frac{Y_i}{W_i} \tag{IV}$$

In the latter group of equations, t is the time, x is the spatial coordinate, $A(x)$ is the spatially variable cross-sectional area – which is constant in these cases - ρ is the mass density, v the velocity, p^0 the thermodynamic pressure and T the temperature; Y_i is the mass fraction of species i, and $j_i=\rho Y_i V_i$ its diffusion flux; here V_i denotes the diffusion velocity of species i; c_{p_i} and h_i denote the mass-based constant-pressure specific heat and enthalpy, respectively, of species i, and w_i is its mass rate of production; c_p is the mixture's frozen specific heat capacity, and λ is its thermal conductivity. Boundary conditions are applied for the dependent variables: mixture density, ρ, temperature, T and composition Y_i infinitely far upstream and infinitely far downstream of the flame. Located far upstream of the flame is the cold boundary; here the respective numerical values prevailing in the fresh unburnt mixture are to be prescribed. Located far downstream of the flame is the hot boundary; here the equilibrium composition prevails at an implicitly given temperature.

Upon defining the vector of dependent variables,

$$u=(Y_1,...,Y_n,T,\rho,v)^T \tag{IV}$$

The above mentioned system can then be cast into the general form,

$$B(u)\frac{du}{dt}=f(u) \tag{V}$$

In previous studies [11], different methods for the calculation of flammability limits were evaluated based on their capacity to capture different aspects of flame extinction. One of the conclusions at the time is that spherical geometries marginally improve the planar flame calculations of the above mentioned limits. Despite this, influence of such methods in the calculation of laminar burning velocities (which is the parameter of interest in this work) is not assessed therein.

Consequently, here, two different flame geometries are used and compared: 1D freely propagating flame and 1D spherically expanding flame. The temperature and the species mole fractions are specified at the cold boundary, while zero gradients are imposed in the hot boundary. A hybrid time-integration/Newton technique is adopted to solve the steady state equations for the planar geometry and the Euler method is used in

the spherical case. In both geometries stoichiometric mixtures of hydrogen/air are modeled and a 21-step kinetic mechanism is used [12].

In the spherical case the constant-pressure limiting case is considered. Initially, the entire system is at 300 K except at the centre where a hotspot is located that triggers the ignition. As a result additional boundary conditions are defined and they concern essentially to the centre of the system. An initial temperature profile is defined according to Figure 1. Again in the centre symmetry conditions are imposed for all dependent variables. This means, that at the coordinate origin, at all times including the initial time, the radial velocity component is zero, and that temperature and species mole fractions have zero gradients there.

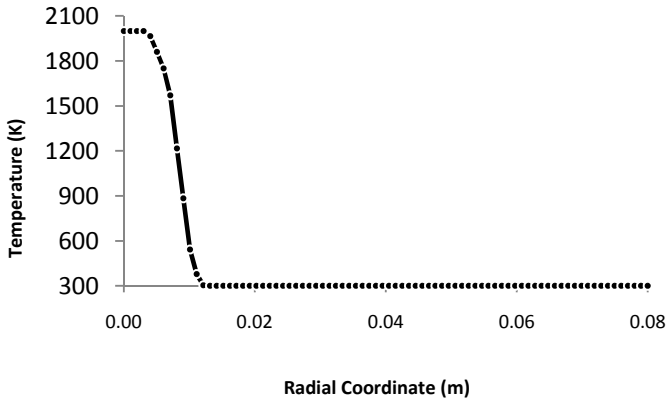

Figure 1: Initial temperature profile adopted in the spherical case

Hotspot value

Figure 2 shows an initial profile with a 2000 K hotspot in the origin decreasing dramatically to 300 K within 8mm length. This ‘step’ measures approximately one tenth of the total radius of the domain. Several hotspots were computed as it can be seen in Figure 2, thus every flame front becomes almost coincident after running 260 timesteps (which takes about 3 minutes in a standard dual core pc). Consequently the hotspot value has no influence on the laminar burning velocity values.

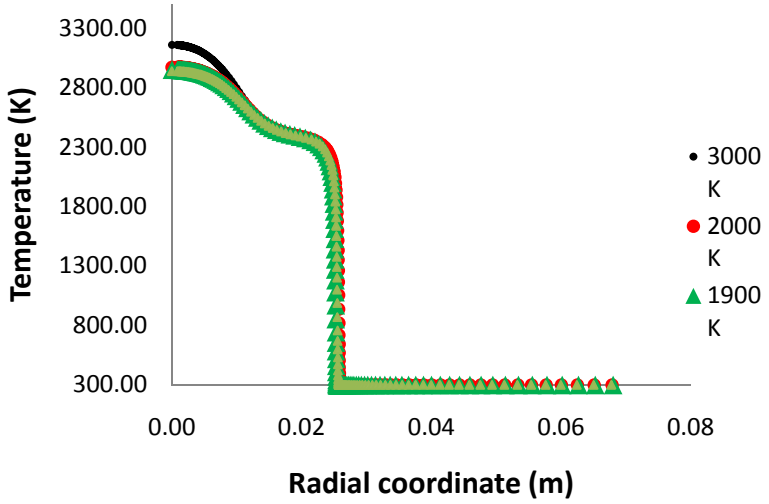

Figure 2: Computed temperature profiles for the spherical case of stoichiometric H_2/air mixture, for 260 timesteps. Four different hotspot temperatures (3000 K, 2000 K, 1900 K and 1850 K).

Domain size/Grid points and Radius of the initial profile

Figure 3 shows four computed cases with the same maximum temperature in the initial temperature profile (2000 K), although with different domain sizes, number of grid points and radius of the initial profile. Figure 3 reports that all the flame fronts have coincident slopes. One of flame fronts shows an offset of approximately 8mm because the initial temperature profile used is double sized. For these four cases, the laminar burning velocities are approximately the same and the value is around 2.55 m/s.

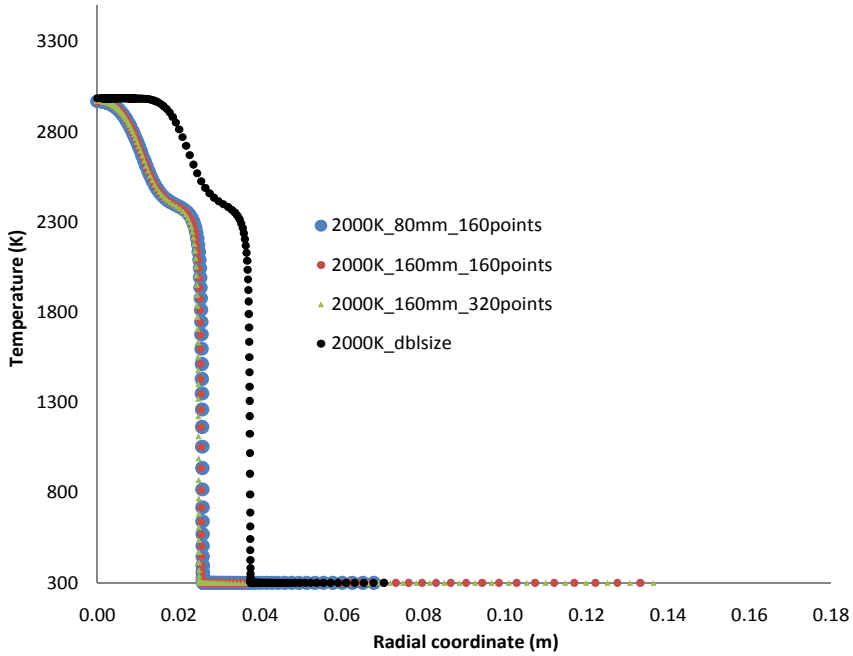

Figure 3: Computed temperature profiles for the spherical case of stoichiometric H_2/air mixture, for 260 timesteps. Different domain sizes (80 mm and 160 mm) are computed, as well as different number of grid points (160 and 320) and also the radius of the initial temperature profile (~16 mm).

Figure 4 shows that the planar geometry (or freely propagating flame – FP) represents more accurately the trend observed in the experimental data [13]. The average deviation for the spherical geometry is 15.3% against 11.2% in the FP case. In the spherical case the maximum burning velocity is shifted to leaner compositions, more precisely, to a hydrogen volume fraction of 37.08% when a value of 3.31 m/s is achieved. For the planar geometry the highest value is achieved for a mixture with 41.71% of H_2 and its value is 3.06 m/s. The latter scenario is more coherent with the experimental trend and the deviation to the experimental peak is around 6.7%.

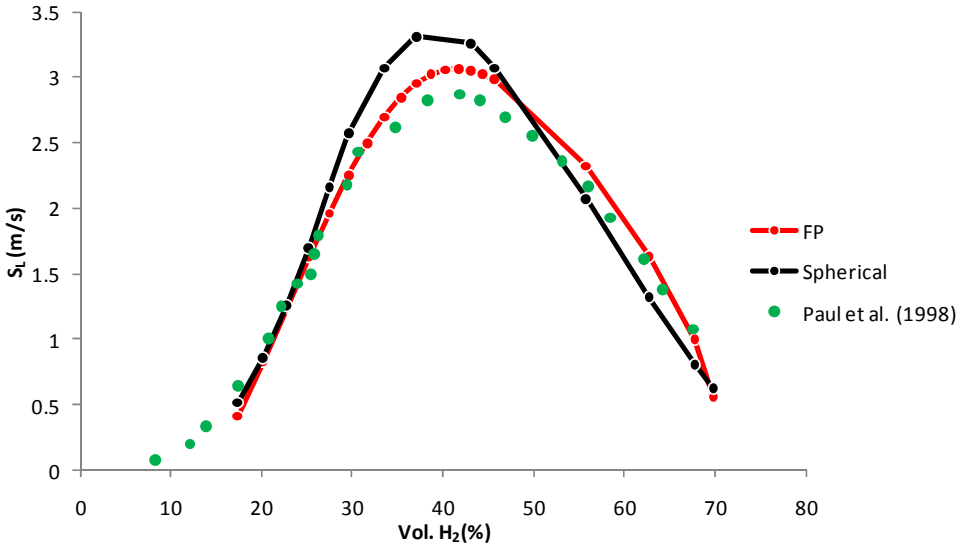

Figure 4: Computed laminar burning velocities for the spherical case and for the freely propagating (FP)/ planar (lines) and experimental values (points) [13].

3 H_2 RESULTS

Figure 5 shows four different models and their laminar burning velocities compared against a set of experimental data [13-15]. Models differ from each other due to the kinetic mechanism used. Since hydrogen reaction steps can be found in hydrocarbon mechanisms (such as CH_4), several "sub-mechanisms" for hydrogen can therein be extracted and studied. In this work, four kinetic mechanisms are compared [12, 16-18]:

1. GRI 2.11 contains 277 elementary chemical reactions and 49 species [16]. It is not optimized for modelling pure nitrogen-hydrogen-oxygen chemistry or any form of NO_x removal process.
2. Konnov mechanism version 0.5 is a set of 1200 reactions and 127 species [18]. The mechanism includes much more than methane (or natural gas) oxidation reaction set. It also includes the combustion of C_2-C_3 hydrocarbon species and their derivatives, N-H-O chemistry and in-flame NO_x formation.
3. Q-Mech is a set of 463 reactions and 117 species [17]. It is a kinetic mechanism optimized for propane.
4. San Diego contains 21 reactions and 10 species [12]. It is specially optimized for hydrogen combustion.

The differences between each mechanism rely essentially on the number of reactions and the value of rate parameters. Besides this, Konnov mechanism differs from other mechanisms because the initiation step is assumed to be the collision of H_2 and O_2 molecules to produce two OH radicals. Although it has now been shown that this collision is extremely unlikely and not fast enough to be important [19]. As can be seen in Figure 5 this main difference does not influence the prediction of laminar burning velocities.

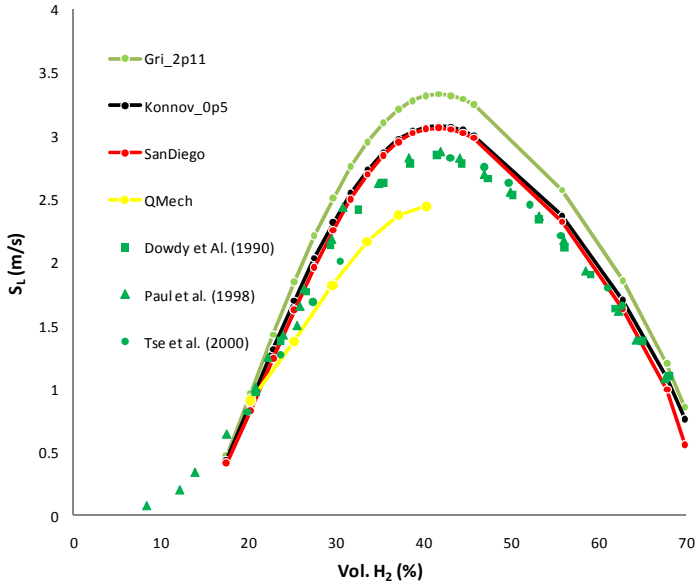

Figure 5: Measured and calculated laminar flame speeds. Solid lines, models from this work (with different kinetic mechanisms) and points, from different experimental works [13-15].

All the mechanisms can predict the overall trend of the experimental values, including the maximum burning velocity which occurs for all of them at an equivalence ratio of 1.7 (corresponding to 41.7% volume fraction of hydrogen).

Concerning to average deviations the mechanisms can be splitted into two groups. The average deviation of GRI 2.11 is 14.3% and QMech is around 14.4% and they constitute the first group with the worst overall results. However they have the lowest deviations for very lean hydrogen mixtures (Φ=0.6) with 4.4% and 9.8% respectively.

The second group contains Konnov 0.5 and San Diego with an average deviation of 8.6% and 9.0%, respectively. Our numerical investigations show that these are the best mechanisms for the global range of possible mixtures, with an additional attractive for San Diego as it just has 21 reactions. From all of them, San Diego presents the most feasibility for future CFD analysis of hydrogen combustion.

4 H_2 + CO RESULTS

Laminar burning velocities of synthesis gas (or syngas) are analyzed in this section. This mixed gas is often used as an intermediate in the production of other chemical compounds or as a fuel source itself. In practical engineering terms most of it arises from the gasification of coal. The mixture consists primarily of hydrogen, carbon monoxide and sometimes also carbon dioxide.

Figure 6 shows the computed laminar burning velocities for mixtures of syngas without carbon dioxide while in Figure 7 the carbon dioxide dilution effect is shown. In Figure 6 three mixtures are presented with three different volumetric proportions of H2:CO (50%, 25% and 5% of H2). The computed data is then compared with two sets of experimental data [20] and [21]. All the computations included in Figure 6 and Figure 7 were achieved using Davis et al. mechanism (also called CMech) [22].

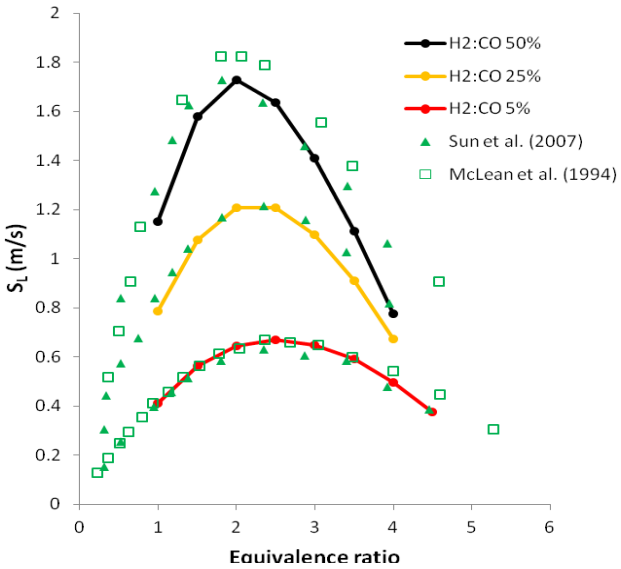

Figure 6: Calculated laminar burning velocities for a stoichiometric mixture of H_2 and CO (solid lines) using Davis et al. mechanism (CMech) [22]. Experimental values taken from [20, 21].

Figure 6 shows that when hydrogen content is lowered (25% and 5%) the peak burning velocity is shifted to richer mixtures (Φ=2.5 instead of Φ=2). This behaviour is observed in the computations (Figure 6) with the average deviations for the maximum predicted burning velocities for the 50%, 25% and 5% mixtures being 1.7%, 0.0% and 6.7%, respectively. Indeed the overall average deviations are 8.7%, 5.4% and 5.4%, respectively.

These results allowed the usage of the same mechanism (CMech) [22] for the evaluation of the carbon dioxide effect which is shown in Figure 7.

Figure 7 shows that syngas laminar burning velocities decrease almost linearly with an increasing content of carbon dioxide in the mixture. The average reduction is 9.1% when considering the transition from 0% to 5% (first two curves of Figure 7) and is 10.3% when the CO_2 content is increased from 5 to 10%.

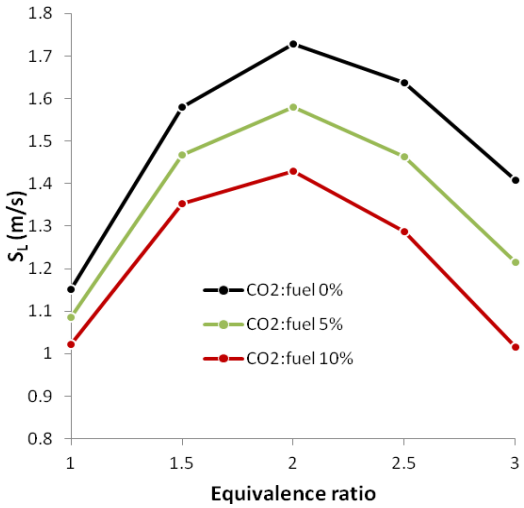

Figure 7: Calculated laminar burning velocities for three stoichiometric syngas mixtures (Φ=1) with 3 different volumetric proportions of CO_2 (0%, 5% and 10%). Fuel in this figure stands for H_2+CO, with volumetric proportions of 50:50. CMech is used [22].

5 $CH_4 + H_2$ results

Figure 8 shows the computed laminar burning velocities for pure methane as a function of the equivalence ratio (Φ). Four different kinetic mechanisms are compared:

1. GRI 3.0 is and optimized version [23] of GRI 2.11 for the natural gas combustion. The new mechanism contains 325 reactions (3 are duplicates because the sum of two rate parameter expressions is required) and 53 species (including argon).
2. Appel mechanism is a set of 544 reactions and 101 species [24]. This mechanism predicts well the major, minor and aromatic species up to pyrene in laminar premixed flames of ethane, ethylene and acetylene fuels at 1bar. There also exists a modification of this mechanism for 10 bar.
3. Konnov 0.5 mechanism [18] has already been described in a previous section.
4. Peters mechanism [25] is a 4-step reduced mechanism.

Figure 8 shows that the reduced mechanism [25] yields poor results with average deviation of 71.4% and with an offset in the predicted peak burning velocity. The maximum computed value with this mechanism is obtained for an equivalence ratio of 1.3 while the experiments [26] show that it occurs for the ratio of 1.1.

So far, Figure 8 also shows that Konnov 0.5 [18] is the best mechanism for predicting laminar burning velocities of pure methane mixtures with an average deviation of 8.5%. Appel [24] and GRI 3.0 [23] have average deviations of 29.0 and 12.9%, respectively.

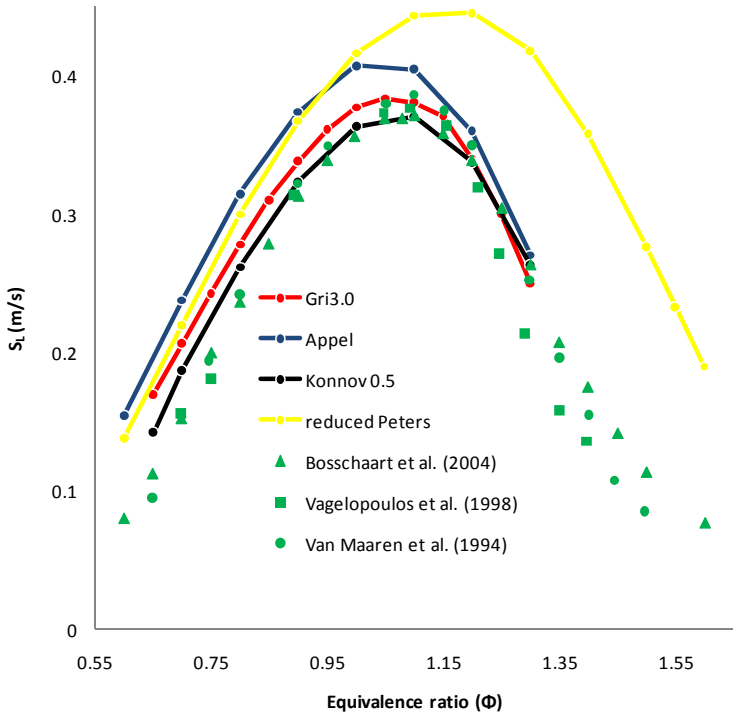

Figure 8: Computed laminar burning velocities of methane-air mixtures against the equivalence ratio (solid lines). Different kinetic mechanisms are shown. Experimental values (points) from [26-28].

Additionally, the effect of variation of hydrogen content is plotted in Figure 9. Two kinetic mechanisms are analyzed here:

1. Konnov 0.5 reduced is derived from the original base mechanism [18]. All C_3-C_6 species other than C_3H_8 and n-C_3H_7 are removed, as well as all nitrogen chemistry, leading to a reduced mechanism with 456 elementary reactions among 54 species [11].
2. QMech [17] has already been described in a previous section.

These mechanisms are chosen to investigate not only the effect of different reaction rate parameters, but also of a different species set. The laminar burning velocities of stoichiometric methane-hydrogen-air mixtures against the volumetric hydrogen content are shown in Figure 9. Large discrepancies are found between two sets of data [1] and [29], namely in the hydrogen rich side (Vol. $H_2 \geq 60\%$). For comparison Ilbas et al. [29] set is considered as the best available as it is the most recent.

The behavior of the above mentioned mixtures can be divided into two different regimes: the first for Vol. H_2 <60% and the second for Vol. $H_2 \geq 60\%$. In the first regime a linear increase in laminar burning velocity is observed with increasing hydrogen content while in the latter a trend of exponential enhancement is observed (Figure 9). Therefore the performance of kinetic mechanisms is also splitted: QMech [17] mechanism predicts better the velocities in the hydrogen-poor side and Appel [24] is the best for the hydrogen-rich side (Figure 9). The average deviation of QMech in the poor side is 10.0% whereas the same parameter for Appel in the rich side is 24.3%.

This latter value for hydrogen-rich mixtures is high and the prediction of the exponential increase in the velocity due to relative higher quantities of hydrogen in the mixtures remains a challenge for further study.

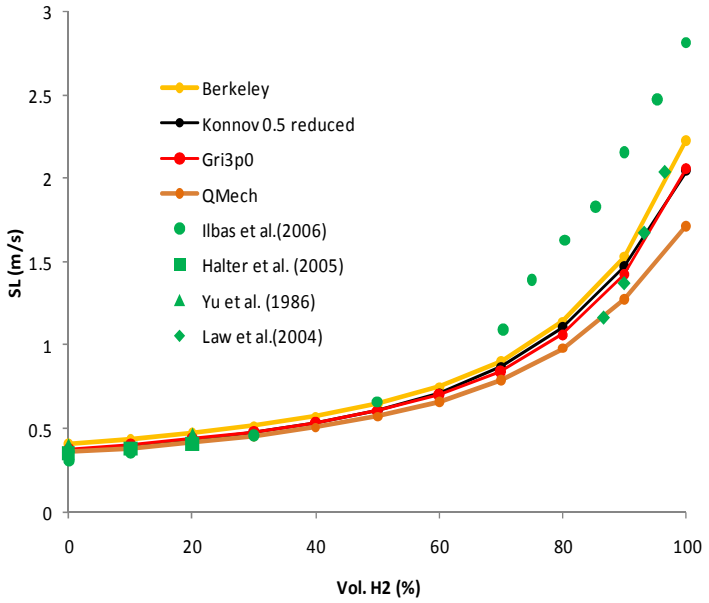

Figure 9: Computed laminar burning velocities of stoichiometric methane-hydrogen-air (Φ=1) mixtures against the volumetric percentage of hydrogen in the mixture (solid lines). Different kinetic mechanisms are shown. Experimental values from [1, 29-31].

6 C_3H_8 + H_2 results

Propane is the major component of the liquid petroleum gas and has a good air-fuel mixing potential. Other advantage is that it can be stored in liquid phase under moderate pressures. These properties motivated several authors to undertake experimental studies on propane-air mixtures [13, 27, 32, 33]. However, to the best of the author's

knowledge, only a reduced number of people concerned with the ternary blend of propane-hydrogen-air, which is the focus of this part of our work. The computed laminar burning velocities of propane-air mixtures are shown in Figure 10, while in Figure 11 the same computed quantities are presented for propane-hydrogen-air mixtures.

From Figure 10 it turns out that two experimental sets of data [13, 27] have large discrepancies between each other. These discrepancies arise from the experimental method used. However the performance of Konnov mechanism [18] was optimized against the latter set of data [27] , so that trend is assumed here also as the comparison basis. Evidence in Figure 10 also indicates that the reduced Konnov mechanism [11] shows reasonable accordance with the Konnov 0.5 base mechanism (deviations not greater than 3%), only in the lean side ($\Phi<0.9$). However in the rich side, namely, for $\Phi=1.4$, the average deviation achieved with the reduced mechanism is 13% higher than that Konnov 0.5 base mechanism. As stated in previous section the reduced Konnov mechanism is obtained by eliminating reaction steps involving nitrogen and all C_3-C_6 species other than C_3H_8 and n-C_3H_7.

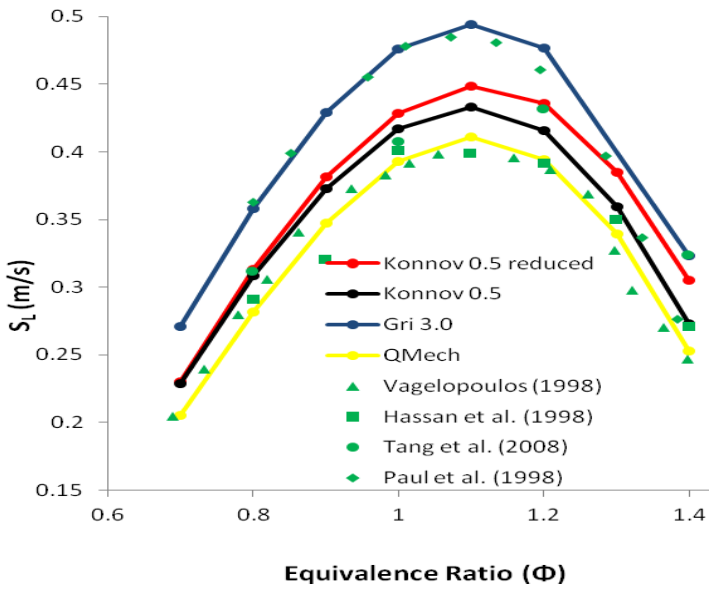

Figure 10: Computed laminar burning velocities of propane-air mixture against the equivalence ratio (Φ) – solid lines. Different experimental sets of data (points) are used for comparison [13, 27, 32, 33].

Besides this evidence, Figure 10 also showed that QMech is the best mechanism to predict propane laminar burning velocities with an average deviation of 3.5%. The same deviation for GRI 3.0 is 26.3%, while for Konnov 0.5 reduced is 12.9% and Konnov 0.5 standard mechanism is 8.2%. As a result, this group of reaction mechanisms is used to extend this study to propane-hydrogen-air mixtures (Figure 11).

Figure 11 shows that several blends of propane and hydrogen always reach their maximum laminar burning velocities at a unity equivalence ratio ($\Phi=1$) independently of the relative quantities between the fuels. Apparently Figure 11 also shows that almost all leaner mixtures ($\Phi \leq 1$) have better agreement with experimental results than richer ones ($\Phi > 1$). Anyway, as Figure 11 shows a great number of mixtures a summary of all the average deviations is summarized in Table 1.

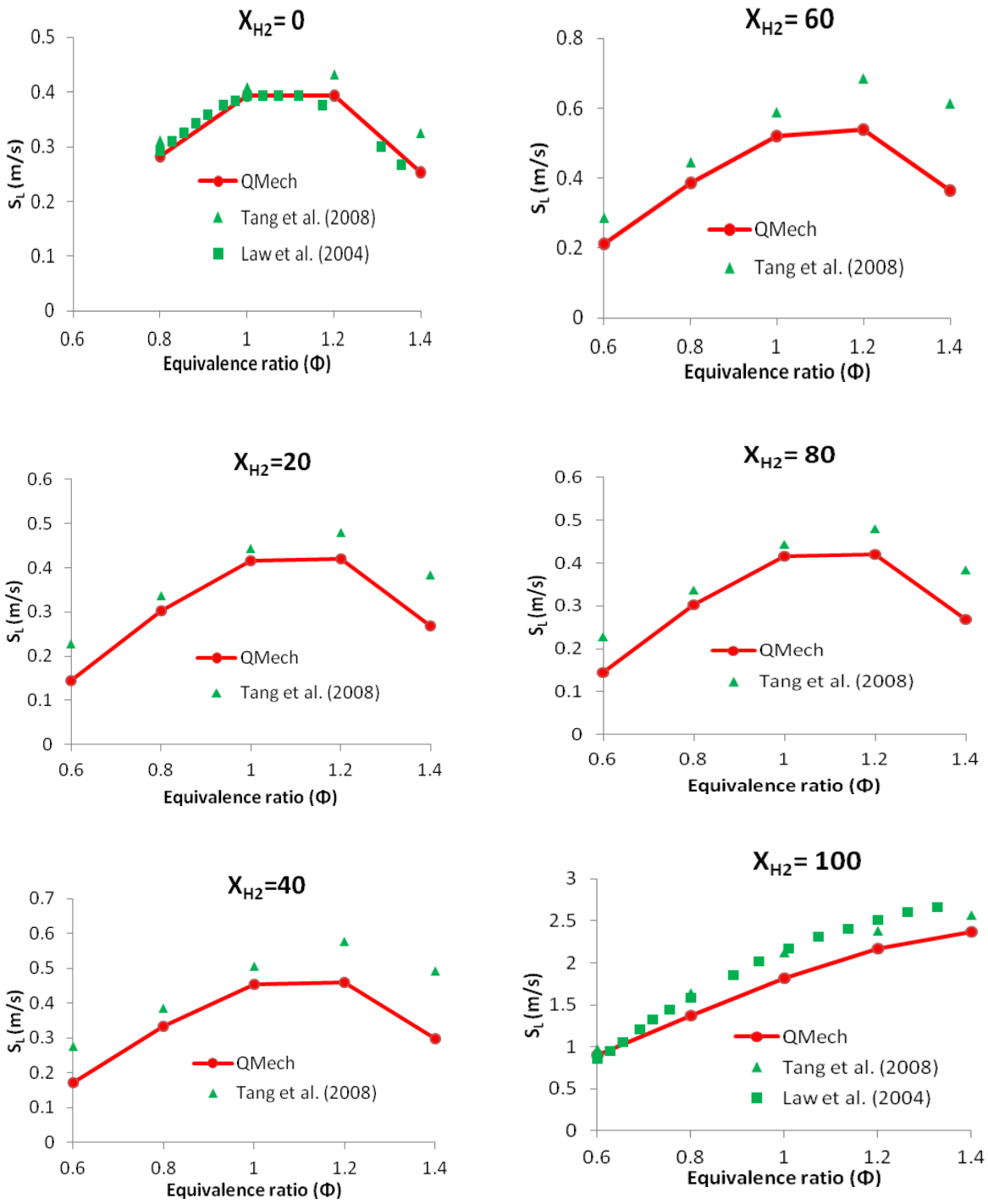

Figure 11: Computed laminar burning velocities of several propane-hydrogen-air mixtures vs. the equivalence ratio (solid lines). Different plots represent different volumetric quantities of hydrogen in the mixture. Experimental values (points) extracted from [1, 33].

V_{H2} (%)	$\Delta_{\Phi= 0.6\text{-}1}$ (%)	$\Delta_{\Phi= 0.6\text{-}1.4}$ (%)
100	12.7	11.1
80	8.0	9.3
60	16.9	22.5
40	20.5	24.3
20	17.8	19.3
0	6.8	11.1

Table 1: Average deviations (Δ(%)) for all the propane-hydrogen-air mixtures shown in Figure 11. Two deviations are calculated for different ranges of equivalence ratios.

It is important to note that two average deviations are calculated for each mixture in Table 1. An average deviation for the mixtures within the range $0.6 \leq \Phi \leq 1$ and another deviation for the all range $0.6 \leq \Phi \leq 1.4$. For blends of propane-hydrogen-air mixtures ($20\% \leq VH2 \leq 80\%$) the average deviations for leaner mixtures is always smaller than the overall deviation. However the mixture with an 80% of hydrogen presents the best agreement with experimental results (under 10%). All other mixtures show higher deviations. Despite this, the results can feed further research on the understanding of the effects of molecular transport phenomena in laminar flames.

7 CONCLUSIONS

It is found that for H_2-air-mixtures:

- the best kinetic mechanism to predict the laminar burning velocities is San Diego with its 21 elementary reactions. As the number of steps is reduced the potential use of this mechanism in further CFD analysis builds-up an additional advantage.

It is found for H_2+CO mixtures:

- the CMech predicts the laminar burning velocities with reasonable agreement.
- that the increasing quantities of carbon dioxide in these mixtures linearly decrease laminar burning velocities.

It is found for CH_4-air mixtures:

- the best kinetic mechanism to predict the laminar burning velocities is Konnov 0.5.

It is found for CH_4-H_2-air mixtures:

- there are two mechanisms with the best agreement with experiments: QMech for mixtures with low content of hydrogen V_{H2} <60% and Appel for $V_{H2} \geq 60\%$. However in the latter case the average deviation exceeds 20%. Consequently the prediction of this trend remains a challenge for future work.

It is found for C_3H_8-air mixtures:

- the QMech is the best kinetic mechanism to predict its laminar burning velocities.

It is found for C_3H_8-H_2-air mixtures:

- QMech predicts better the laminar burning velocities for leaner mixtures ($0.6 \leq \Phi \leq 1$).
- the peak burning velocity occurs always at an equivalence ratio of 1.0 independently of the relative composition between the fuels.

8 REFERENCES

1. C.K. Law, O.C.K., Effects of hydrocarbon substitution on atmospheric hydrogen–air flame propagation. International Journal of Hydrogen Energy, 2004. 29: p. 867-879.
2. Badin J.S., T.S., Energy pathway analysis—a hydrogen fuel cycle framework for system studies. International Journal of Hydrogen Energy, 1997. 22: p. 389-395.
3. S.P.R. Muppala, M.N., N.K. Aluri, H. Kido, J.X. Wen, M.V. Papalexandris, Experimental and analytical investigation of the turbulent burning velocity of two-component fuel mixtures of hydrogen, methane and propane. International Journal of Hydrogen Energy, 2009. 34: p. 9258-9265.
4. A. N. Lipatnikov, J.C., Lewis number effects in premixed turbulent combustion and highly perturbed laminar flames. Combustion Science and Technology, 1998. 137: p. 277-298.
5. Cassidy, J.F., Emissions and total energy consumption of a multicylinder piston engine running on gasoline and a hydrogen-gasoline mixture. 1977, NASA.
6. F. Van den Schoor, R.T.E.H., J.A. van Oijen, F. Verplaetsen, L.P.H. de Goey, Comparison and evaluation of methods for the determination of flammability limits, applied to methane/hydrogen/air mixtures. Journal of Hazardous Materials, 2008. 150: p. 573-581.
7. D.R.Ballal, A.H.L., The structure and propagation of turbulent flames. Proceedings of the Royal Society of London, 1975. 344: p. 217-234.
8. A. N. Lipatnikov, J.C., Molecular transport effects on turbulent flame propagation and structure. Progress in Energy and Combustion Science, 2005. 31: p. 1-71.
9. Peters, N., Laminar flamelet concepts in turbulent combustion. Symposium (International) on Combustion, 1988. 21: p. 1231-1250.
10. Rogg, B., RUN-1DL: the Cambridge universal laminar flame code. 1991, University of Cambridge
11. F. Van den Schoor, F.V., J. Berghmans, Calculation of the upper flammability limit of methane/air mixtures at elevated pressures and temperatures. Journal of Hazardous Materials, 2008. 153: p. 1301-1307.
12. Williams, F.A. 2005 [cited; Available from: http://maeweb.ucsd.edu/~combustion/cermech.
13. P. Paul, J.W., A re-evaluation of the means used to calculate transport properties of reacting flows. Symposium (International) on Combustion, 1998. 27: p. 495-504.

14. D. R. Dowdy, D.B.S., S. C. Taylor, A. Williams, The use of expanding spherical flames to determine burning velocities and stretch effects in hydrogen/air mixtures. Symposium (International) on Combustion, 1991. 23: p. 325-332.
15. S.D. Tse, D.L.Z., C.K. Law, Morphology and burning rates of expanding spherical flames in H2/O2/inert mixtures up to 60 atmospheres Symposium (International) on Combustion, 2000. 28: p. 1793-1800.
16. C.T. Bowman, R.K.H., D.F. Davidson, W.C. Gardiner, Jr., V. Lissianski, G.P. Smith, D.M. Golden, M. Frenklach and M. Goldenberg. [cited; Available from: http://www.me.berkeley.edu/gri_mech/.
17. Z. Qin, V.V.L., H. Yang, W. C. Gardiner, S. G. Davis, H. Wang, Combustion chemistry of propane: a case study of detailed reaction mechanism optimization Proceedings of the Combustion Institute, 2000. 28: p. 1663-1669.
18. Konnov, A.A. Detailed reaction mechanism for small hydrocarbons combustion. 2000 [cited; Release 0.5:[Available from: http://homepages.vub.ac.be/~akonnov/.
19. J.V. Michael, J.W.S., L.B. Harding, A.F. Wagner, Initiation in H2/O2: rate constants for H2 + O2 - H + HO2. Proceedings of the Combustion Institute, 2000. 28: p. 1471-1478.
20. Hongyan Sun, S.I.Y., G. Jomaas, C.K. Law, High-pressure laminar flame speeds and kinetic modelling of carbon monoxide/hydrogen combustion. Proceedings of the Combustion Institute, 2007. 31: p. 439-446.
21. I.C. McLean, D.B.S., S.C. Taylor, The use of carbon monoxide/hydrogen burning velocities to examine the rate of the CO+OH reaction. Proceedings of the Combustion Institute, 1994. 25: p. 749-757.
22. S. G. Davis, A.V.J., H. Wang, F. Egolfopoulos, An optimized kinetic model of H2/CO Combustion. Proceedings of the Combustion Institute, 2005. 30: p. 1283-1292.
23. Smith, G.P.G., D. M.; Frenklach, M.; Moriarty, N. W.; Eiteneer, B.; Goldenberg, M.; Bowman, C. T.; Hanson, R. K.; Song, S.; Gardiner, W. C., Jr.; Lissianski, V. V.; Qin, Z. . [cited; Available from: http://www.me.berkeley.edu/gri_mech/.
24. J. Appel, H.B., M. Frenklach, Kinetic Modelling of Soot Formation with Detailed Chemistry and Physics: Laminar Premixed Flames of C2 Hydrocarbons. Combustion and Flame, 2000. 121: p. 122-136.
25. F. Mauss, N.P., B. Rogg, F.A.Williams, Reduced kinetic mechanisms for premixed hydrogen flames, in Reduced kinetic mechanisms for applications in combustion systems. 1993. p. 29-43.
26. K.J. Bosschaart, L.P.H.d.G., The laminar burning velocity of flames propagating in mixtures of hydrocarbons and air measured with the heat flux method. Combustion and Flame, 2004. 136: p. 261-269.
27. C.M. Vagelopoulos, F.N.E., Direct experimental determination of laminar flame speeds. Symposium (International) on Combustion, 1998. 27: p. 513-519.
28. A. Van Maaren, D.S.T., L. R. H. De Goey, Measurement of Flame Temperature and Adiabatic Burning Velocity of Methane/Air Mixtures. Combustion Science and Technology, 1994. 96: p. 327-344.
29. M. Ilbas, A.P.C., I. Yılmaz, P.J. Bowen, N. Syred, Laminar-burning velocities of hydrogen–air and hydrogen–methane–air mixtures: An experimental study. International Journal of Hydrogen Energy, 2006. 31: p. 1768-1779.
30. F. Halter, C.C., N. Djebaili-Chaumeix, I. Gokalp, Characterization of the effects of pressure and hydrogen concentration on laminar burning velocities of

methane–hydrogen–air mixtures. Proceedings of the Combustion Institute, 2005. 30: p. 201-208.

31. Yu G., L.C., Wu CK., Laminar flame speeds of hydrocarbon+air mixtures with hydrogen addition. International Journal of Hydrogen Energy, 1986. 63: p. 339-347.
32. M.I. Hassan, K.T.A., O.C. Kwon, G.M. Faeth, Properties of Laminar Premixed Hydrocarbon/Air Flames at Various Pressures. Journal of Propulsion and Power, 1998. 14: p. 479-488.
33. C. Tang, Z.H., C. Jin, J. He, J. Wang, X. Wang, H. Miao, Laminar burning velocities and combustion characteristics of propane–hydrogen–air premixed flames. International Journal of Hydrogen Energy, 2008. 33: p. 4906-4914.